

Helium Catalyzed D-D Fusion in a Levitated Dipole

J. Kesner, D.T. Garnier[†], A. Hansen[†], M. Mauel[†], L. Bromberg

Plasma Science and Fusion Center, MIT, Cambridge, Mass. 02139

[†]Dept. Applied Physics, Columbia University, New York, N.Y. 10027

PACS 28.52.-S

Abstract

Fusion research has focused on the goal of a fusion power source that utilizes deuterium and tritium (D-T) because the reaction rate is relatively large. Fusion reactors based on the deuterium-deuterium (D-D) reaction however, might be superior to D-T based reactors in so far as they minimize the power produced in neutrons and do not require the breeding of tritium. We explore an alternative D-D based fuel cycle and show that a levitated dipole may be uniquely suited for this application. We find that a dipole based D-D power source can potentially provide a substantially better utilization of magnetic field energy with a comparable mass power density to a D-T based tokamak power source.

1 Introduction

During the past several decades the focus of controlled fusion research has been the development of magnetic traps that are appropriate for igniting and sustaining a controlled fusion burn. The fusion cross section and reaction rate coefficient is significantly larger for deuterium-tritium (D-T) than any other reaction which makes a D-T based power source easier to ignite and burn than any other fusion power source. The D-T rate coefficient is two orders of magnitude larger than the rate coefficient for Deuterium-³Helium (D-³He) reaction or for the deuterium-deuterium (D-D) reaction. The tokamak has proven to be the most successful device for producing near-ignition plasma conditions and much of the research in this area has focused on tokamaks. For these reasons it seems likely that the first self-sustaining fusion reactor will utilize D-T fuel in a tokamak.

In this article we propose a different approach for a fusion power source, based on an alternative fuel cycle which we call “helium catalyzed D-D”. The D-D cycle is difficult in a traditional fusion confinement device such as a tokamak because good energy confinement is accompanied by good particle confinement which leads to a build up of ash in the discharge [1]. Recently there has been a developing interest in the confinement of a plasma in a levitated dipole configuration [2, 3] and a levitated dipole experiment known as LDX is presently under construction [4]. A dipole may have the unique capability of producing excellent energy confinement accompanied by low particle confinement. We will explore the application of a levitated dipole as a D-D power source.

The basis for this behavior is the MHD prediction that a dipole confined plasma remains stable below a critical pressure gradient. At marginal stability, which occurs when $pU^\gamma = \text{constant}$ with p the plasma pressure, U the differential flux tube volume $U \equiv \oint dl/B$ and $\gamma = 5/3$ an exchange of flux tubes does not modify the pressure profile [5, 6]. When flux tubes exchange adiabatically the plasma cools as it moves into lower fields and heats as it

moves into higher fields and at marginality it remains in thermal equilibrium with the local pressure as it circulates. Non-linear studies indicate that large scale convective cells will form when the MHD stability limit is violated, which result in rapid circulation of plasma between the hot core and the cooler edge [7, 8, 9].

A properly designed dipole power source would ignite while maintaining MHD stability. Once it ignites we expect the pressure gradient to violate the interchange stability criterion which will lead to the formation of convective cells that circulate particles between the core and edge region. The convective cells also unload excess heat so as to maintain a pressure profile that is close to the marginal state.

Theoretical studies predict that a levitated dipole can support high beta plasmas and this translates into excellent magnetic field utilization. Studies also predict that the confined plasma can be stable to low frequency (drift wave) modes and therefore we might expect that the energy confinement will remain close to the classical value. Additionally a levitated dipole device would be intrinsically steady state and extract power as surface heating, permitting a thin walled vacuum vessel and eliminating the need for a massive neutron shield.

By way of comparison, burning D-T entails several difficulties. As tritium does not occur naturally it must be bred (using the $n(^6\text{Li}, T)\alpha$ reaction) and providing a sufficient breeding ratio (> 1) poses a serious challenge for plant design [10]. In addition, tritium is bioactive and is subject to radioactive decay and so tritium handling complicates the operation of such a device. A second difficulty is posed by the production of 14.1 MeV neutrons, the product of the D-T fusion reaction. Energetic neutrons will degrade, damage and activate the structural materials of the reactor. Furthermore, the large mass that is required to stop energetic neutrons leads to the requirement that a massive blanket and shield must surround the fusing D-T plasma and be internal to the superconducting toroidal field coils.

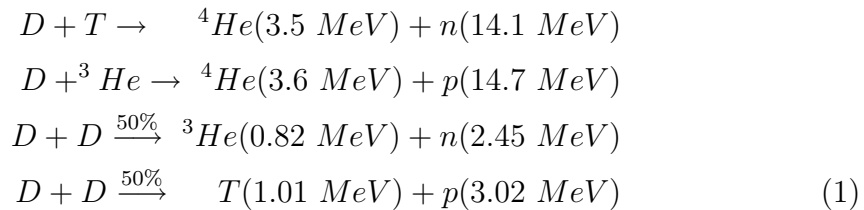
The D-³He reaction eliminates most of the energetic neutron generation. The use of a dipole for burning D-³He as both a power source [3] and for propulsion [12] has been examined. However, as with tritium, ³He is not abundant on the earth. It has been pointed out that it can be mined on the moon [13] or on a longer time scale be obtained from Jupiter [14] but developing the required technology for non-terrestrial mining presents a daunting task.

The D-D reaction is perhaps the most interesting from the point of view of eliminating both the tritium and the energetic neutron problems. However the relatively small fusion cross section has made this approach problematical.

In this study we show that a levitated dipole device may be ideally suited for a D-D based fusion power source. Section 2 reviews fusion reaction considerations and dipole physics. In Sec. 3 we present as a conceptual dipole configuration that can serve as an example of the plasma and plant parameters considered. Section 4 presents the conceptual configuration for a small D-T based ignition experiment that might serve as a crucial test of the approach and Sec. 5 presents a discussion of this approach. Conclusions are presented in Sec. 6.

2 D-D Fusion

The most important reactions for controlled nuclear fusion are as follows:



D-T and D-³He require difficult-to-obtain fuels whereas the D-D cycle utilizes only deuterium for fuel, which can be easily extracted from sea water.

Unfortunately the low fusion reaction rate requires exceptionally good confinement for ignition. Furthermore the particle to energy confinement time ratio, τ_p^*/τ_e is a sensitive parameter for the ignition of a D-D system and remains relatively constant in currently studied systems because both particle and energy confinement derive from the same underlying process of micro-turbulence. Studies show [1] that ignition requires $\tau_p^*/\tau_E < 2$ whereas tokamak experiments generally observe $\tau_p^*/\tau_E > 5$. Ignition of D-D fuel therefore requires a system that can decouple the particle and energy confinement. This requirement suggests the use of a closed-field-line system like a dipole in which large scale convective cells can rapidly convect particles out of the fusing plasma core. (In a properly designed system the plasma is quiescent up to the point of ignition. Thereafter the large internal power production would give rise to instability that leads to the formation of convective cells which would serve to maintain the pressure profile at close to a critical value.)

Referring back to the fusion reactions shown in Eq. (1) there are two equally likely D-D fusion reactions. The first reaction produces a ^3He whereas the second produces a triton. The ^3He will fuse with the background deuterium. Permitting the tritium to fuse leads to the "catalyzed DD" fuel cycle. However because the D-T reaction would produce an energetic (14.1 MeV) neutron that would be difficult to prevent from entering and heating an internal coil, we propose to remove the triton before a substantial fraction can fuse and replace it with the ^3He tritium decay product. This leads to the production of 22 MeV of energy per D-D fusion reaction. This fusion cycle has been discussed in References [11, 15] and will be referred to as "Helium catalyzed D-D" fusion.

The Lawson criterion is obtained by balancing the fusion power that is produced in energetic ions (which can self-heat the plasma) with Bremsstrahlung radiation and with energy transport losses characterized by a confinement time, τ_E . We will assume that we can extract the tritium produced in the D-D reaction and reinject the ^3He decay product into the plasma. In equi-

librium the deuterium density is determined from the following balance:

$$\frac{d n_D}{dt} = 0 = S_D - n_D^2 \langle \sigma v \rangle_{DD} - n_D n_T \langle \sigma v \rangle_{DT} - \frac{n_D}{\tau_p}. \quad (2)$$

with S_D the deuterium source and τ_p the particle confinement time. For simplicity we will assume that all ions have a similar confinement time and later discuss the implications of selectively removing tritium. The ^3He density is then determined from the following rate equation:

$$\frac{d n_{He3}}{dt} = 0 = \frac{1}{4} n_D^2 \langle \sigma v \rangle_{DD} + \frac{n_T}{\tau_p} - n_{He3} n_D \langle \sigma v \rangle_{DHe3}, \quad (3)$$

and the tritium density is obtained from the rate equation,

$$\frac{d n_T}{dt} = 0 = \frac{1}{4} n_D^2 \langle \sigma v \rangle_{DD} - n_D n_T \langle \sigma v \rangle_{DT} - \frac{n_T}{\tau_p}. \quad (4)$$

These equations will determine the fraction of the non-deuterium ions, which are found to be low compared with the deuterium density. Finally the power balance will yield;

$$\begin{aligned} & \frac{\frac{3}{2} n_e T_e + \frac{3}{2} (n_T + n_D + n_{He3}) T_i}{\tau_E} + n_e^2 P_{Brem}(T_e) \\ & = \frac{1}{2} n_D^2 \langle \sigma v \rangle_{DD} E_{DD} + n_D n_{He3} \langle \sigma v \rangle_{DHe3} E_{DHe3} + n_D n_T \langle \sigma v \rangle_{DT} E_{DT}. \end{aligned} \quad (5)$$

Additionally neutrality requires $n_D + n_T + 2n_{He} = n_e$. The $E_{\alpha\alpha}$ notation in Eq. (5) represents the energy produced in the respective fusion reactions. Setting $T_e = T_i$, assuming a fixed ratio τ_E/τ_p and applying quasi-neutrality ($n_e = n_D + n_T + 2n_{He3}$) we can solve for the equilibrium fraction of each species and formulate the Lawson criterion, $n_e T \tau_E$ vs T . Fig. 1 compares the Lawson criterion for Helium catalyzed D-D fusion for $\tau_E/\tau_p = 5$ with the fusion reactions of Eq.(1). (Later we will see that τ_E/τ_p can greatly exceed this value.) For operation at an ion temperatures of 40 KeV the He-catalyzed-DD cycle presents a favorably low requirement on $n\tau_E T$.

The energetic triton produced in the primary D-D reaction, however, will slow down and thermalize before it can be convected out to the plasma edge

and removed. We can estimate the beam-plasma fusion rate for an energetic triton slowing down in a thermal deuterium plasma. Using the energy loss rate from Ref. [16] and the D-T fusion cross-sections from Ref. [17] we can obtain the fusion probability for a 1 MeV triton in a warm deuterium plasma. The fusion probability as a function of plasma temperature ($T_e = T_i$) is shown in Fig. 2. For a 40 KeV deuterium plasma we find that approximately $\approx 7\%$ of the tritons fuse as they slow down.

2.1 Review of Dipole Physics

The dipole fusion concept was motivated by satellite observations of planetary magnetospheres that show centrally peaked plasma pressure profiles forming naturally when the solar wind drives plasma circulation and heating [2]. In the magnetosphere the primary loss for bulk plasma is flow along field lines into the planetary poles and as a fusion concept we want to eliminate this loss by utilizing a levitated floating coil to maintain the magnetic field. The field lines close around the coil and we will assume that a high beta plasma surrounds the ring. This plasma may be characterized as being divided into two regions: In the “inner” region, $R_c < R < R_p$ with R the flux tube radius on the outer mid-plane, R_c the outer radius of the floating coil cryostat and R_p the radius at the pressure peak. In this region the plasma pressure is close to zero at the ring, $p(R_c) \sim 0$ and rises in a region of “good curvature” to a peak value at $R = R_p$. In the “outer” region $R_p < R < R_w$ with R_w the mid-plane wall radius the pressure falls in a region of “bad curvature” from its peak value to its value on the separatrix as indicated in Fig. 3.

The equilibrium of high beta plasmas follows from the Grad-Shafranov equation and it has been shown that dipole equilibrium can be obtained at all beta values [18, 19, 20]. The plasma in a closed field line system can be stabilized in the outer region of so-called “bad curvature” by plasma compressibility [5, 6]. Figure 4 shows an equilibrium that we shall examine

for a model reactor. In Fig. 4 we have chosen $R_c=9.7$ m, $R_p=10.15$ m, $R_w=30$ m and an edge plasma pressure $p(R_w)=500$ Pa which yields a peak β value of $\beta(R_p)=3.1$.

In magnetohydrodynamic (MHD) theory the stability of interchange modes limits the pressure gradient to a value:

$$d \equiv -\frac{d \ln p}{d \ln U} < \gamma \quad (6)$$

with $U = \oint dl/B$ and γ is the ratio of specific heats ($\gamma \equiv c_p/c_v = 5/3$ is the ratio of specific heats in three-dimensional systems at constant pressure and volume). It has been shown that the interchange criterion is valid for marginal stability at all beta values and that ballooning modes do not limit stability [18, 19, 20]. Recent work utilizing resistive MHD indicates that the usual fractional power resistive modes ($\gamma \propto \eta^{1/3}$) do not appear in a dipole although a weak residual resistive mode may be present that has a growth rate proportional to resistivity, $\gamma_R \propto \eta$ [21].

When the pressure profile exceeds the flute mode stability limit it has been predicted that the system will develop large-scale convective cells which can lead to non-local transport [22, 23, 24, 25, 26]. The non-linear evolution of a hard-core z-pinch (which is a large aspect ratio approximation for a dipole) has recently been studied by Pastukhov [7, 8, 27]. His simulations indicate that when the interchange stability condition (Eq. 6) is violated, large scale convective cells will form that lead to sufficiently large non-local energy transport so as to maintain the system at close to the marginal pressure profile. Additionally he shows that these cells will rapidly convect particles that emanate from a particle source at the plasma edge into the core, leading to a $n_e \propto 1/U$ density profile [28] in the outer dipole region.

Equation (6) indicates that in a bad curvature region the pressure must decay relatively slowly and this implies that ignition in a dipole requires a small plasma in a relatively large vacuum chamber. For a sufficiently large dipole power source, the confined plasma will remain MHD stable as it is

heated to ignition. Once it ignites we would expect the pressure gradient to violate the interchange stability criterion which gives rise to convective cells that will circulate particles between the core and edge region. The convective flow speed has been shown to be ϵc_s with c_s the sound speed and $\epsilon \sim 0.01$ is a small scaling parameter, $\epsilon \approx (\chi/ac_s)^{1/3}$ with χ the thermal diffusivity and a the plasma half width [8]. For an electron temperature $T_e \sim 30$ KeV and $a \sim 10$ m the circulation time of the cells is milliseconds while we will find that the energy confinement time is seconds. The resulting particle confinement time is a fraction of the energy confinement time since particles need only to move a small distance between the outer cell and the plasma edge and tritium can be actively removed from the outer region. Thus tritium and ash can be removed in a time that is a small fraction of the energy confinement time.

For a closed-field line system the MHD stability requirement (Eq.(6)) is intrinsically related to the criteria for the stability of drift waves. If we define the following frequencies:

$$\hat{\omega}_{*p} \equiv \frac{\vec{b} \times \vec{k} \cdot \nabla p}{\Omega_i m_i n_i} \quad (7)$$

and

$$\hat{\omega}_d^{mhd} \equiv \frac{2c}{e} \frac{R k_\theta T}{1 + \gamma \langle \beta \rangle / 2} \frac{\oint dl \kappa / RB^2}{\oint dl / B} \quad (8)$$

with R the cylindrical radial coordinate, κ the field line curvature, k_θ the azimuthal part of the perpendicular wave number ($k_\perp^2 = k_\theta^2 + k_R^2$) and $k_\theta R = m \gg 1$, one can show that d defined in Eq. (6) is equal to $d = \hat{\omega}_{*p} / \hat{\omega}_d^{mhd}$. Therefore the MHD stability requirement, $d \leq \gamma$, (Eq. (6)) can be written as:

$$\hat{\omega}_{*p} = \omega_{*i}(1 + \eta) \leq \gamma \hat{\omega}_d^{mhd}. \quad (9)$$

with ω_{*j} the diamagnetic drift frequency, $\omega_{*j} = T_j \vec{k} \times \vec{b} \cdot \nabla n_0 / (n_j m_j \Omega_j)$ and $\eta = d \ln T / d \ln n$ and Eq. 9 can be shown to lead to the stability of drift frequency modes [30].

It has been shown that the outer region of the dipole can be subject to an “entropy mode” instability when $\eta < 2/3$ [29, 30, 31]. This result holds in all regimes of collisionality [30] and at arbitrary beta [32]. In the inner (good-curvature) region the temperature and pressure will rise moving away from the coil but the density will fall (assuming complete recycle at the internal coil) and therefore $\eta < -1$. In this regime instability of the entropy mode is possible[31]. Ultimately the level of plasma energy transported towards the ring will be determined experimentally and this is one of the goals of the LDX experiment [4].

3 Dipole Based D-D Power Source

We will now consider a dipole based D-D power source. A levitated dipole is intrinsically steady state and leads to a relatively simple reactor configuration. It requires only two large coils, the floating coil and the levitation coil that holds up the floating coil, either from above or below. A third coil may be used to inductively charge the floating coil and small shaping coils may also be utilized as is the case in the LDX experiment [4]. The coils are not inter-locking so that replacement of the floating coil would be a relatively simple procedure.

A dipole fusion source would consist of a relatively small ring in a large vacuum chamber. In the He-catalyzed D-D cycle approximately 92% of the power is generated in energetic ions and a substantial fraction of the plasma energy leaves the plasma as Bremsstrahlung radiation. The surface power loading is relatively low ($< 0.1 \text{ MW}/m^2$) and suggestive of a relatively thin-wall vessel containing a flowing coolant.

The internal floating coil will operate with a high outer surface temperature ($> 1600^0K$) so as to radiate away all of the surface and neutron heating via black body radiation (assuming an emissivity ≈ 1). In addition, we envision that the floating coil will have internal refrigerators that will pump

to the surface the heat that is deposited directly into the superconducting coil via volumetric neutron heating. We imagine that the coil will utilize a high temperature ceramic superconductor such as BSCCO or YBCO [33] capable of operating at a temperature above 50 ⁰K. In the neutronics and thermodynamics studies presented below we will model the coil mass make-up to be similar to BSCCO and assume an operating temperature of 70 ⁰K. Another promising superconducting material is magnesium diboride, which may operate at temperatures of up to 30 ⁰K.

For D-D ignition, the peak pressure $p(R_p)$, must exceed ~ 5 MPa. The power source characteristics for this conceptual study are shown in Table 1 for a floating coil that carries $I_{coil} = 36$ MA with a peak field at the conductor of 30 T (Source A) and for a less aggressive case (same coil dimensions) with $I_{coil} = 25$ MA. (The less aggressive case, Source B, reduces the magnetic hoop stress by 50% to a level which is more compatible with today's magnet technology.) From Eq. (6) the peak-to-edge pressure ratio is:

$$\frac{p(R_p)}{p(R_w)} = \left(\frac{(\oint d\ell/B)_{wall}}{(\oint d\ell/B)_{R_p}} \right)^\gamma \quad (10)$$

For a given size vacuum chamber we have attempted to maximize the fusion power produced. We have chosen a high aspect ratio coil because, at high β , and for a fixed size vacuum chamber, the increased mid-plane field in a high aspect ratio coil more than makes up for the reduced distance to the first wall since $P_{fusion} \propto \beta^2 B^4$.

The plasma parameters were determined by the solution of the Grad-Shafranov equation. We utilize the DIPEQ code [19] and vary parameters to obtain an equilibrium solution that is ignited (fusion power > radiation losses) and produces substantial fusion power (fusion power > 500 MW). The pressure profile which enters into the MHD equilibrium calculation is assumed to be at the marginal level given by Eq. (6), i.e. $p \propto 1/U^\gamma$. We assume that once ignited, convective, non-local energy transport will arise which will clamp the pressure gradient at close to this critical value [8].

	D-D Power Source (A)	D-D Power Source (B)	D-T Ignition
Vac. vessel midplane radius (m)	30	30	8
First wall volume (m^3) †	269	269	21.4
Floating coil major radius (m)	9	9	1.5
Floating coil minor radius (m)	0.7	0.7	0.38
Coil Current (MAT)	35.9	30	15
Peak field at conductor (T)	30	25	26.6
Coil current density (MA/m^2)	330	276	375
Magnet Stored Energy, W_B (GJ)	30.7	21.4	0.62

Table 1: Vacuum chamber and floating coil parameters.

† Assume 4 cm thick vessel with elliptic x-section.

	D-D Power Source (A)	D-D Power Source (B)	D-T Ignition
Peak Plasma Pressure, (MPa)	5.4	4.1	0.55
Peak β	3.1	5.9	3.0
Peak pressure radius, R_p (m)	10.3	10.3	2.4
Peak ion Temp (KeV)	41	37	10.3
Peak electron temperature (KeV)	30	30	10.3
Electron density at R_p (m^{-3})	5.7×10^{20}	4.4×10^{20}	1.8×10^{20}
B field at R_p (T)	2.1	1.5	0.68
Edge Temp (eV)	400	400	300
Edge density (m^{-3})	3.7×10^{18}	3.7×10^{18}	4.6×10^{18}
Fusion Power, P_{fus} (MW)	610	384	12.1
2.45 MeV Neutron Power (MW)	34	21	~ 0
14.1 MeV Neutron Power (MW)	14	8.8	9.73
Bremsstrahlung radiation (MW)	430	362	1.04
Plasma Stored Energy, W_P (GJ)	2.94	2.43	0.015
Engy Confinement time, τ_E^{global} (s)	5.1	6.7	6.6

Table 2: Plasma parameters

To determine the fusion power production we make assumptions including the location of the pressure peak, the edge pressure, the impurity content and the assumed density profile (the pressure profile is specified for the MHD equilibrium calculation). Table 2 indicates the input parameters for the equilibrium calculation. We have assumed $R_p = 10.3 \text{ m}$, an edge pressure of 400 Pa and an oxygen content of 1%. The total stored energy of the plasma decreases as the pressure peak location moved outwards. For example for an increase of the radial location of the pressure peak to $R_p=10.75$ the total power decreases from 610 to 250 MW. The pressure profile and in particular the pressure peak location of an ignited dipole plasma should be self consistently determined by the ratio of energy transport inwards towards the floating coil and outwards towards the first wall. Therefore a proper determination of the pressure peak location would require a detailed knowledge of transport coefficients.

We have utilized the Grad-Shafranov equilibrium to calculate the fusion power profile. The density profile was assumed to have the dependence $n_e \propto 1/U$ [8] up to within 5 m of the plasma edge (near the edge, in the fueling region, we impose a flat density). Thus the core temperature profile has the dependence $T \propto 1/U^{\gamma-1}$. We assume temperature equilibration, ($T_i = T_e$) throughout the plasma profile except where $T_i > 30 \text{ KeV}$. In this region we clamp the electron temperature at $T_e = 30 \text{ KeV}$ because, even though 80% of the fusion power goes into heating the electrons, the copious Bremsstrahlung radiation from the electron channel serves to limit the electron temperature. If we were to assume temperature equilibration throughout the profile the Bremsstrahlung power would rise by 7.2% and the total fusion power fall by 6.9%. Furthermore we have assumed a high wall reflectivity and have ignored synchrotron radiation. Synchrotron radiation would increase the radiated power and could lead to a more stringent ignition condition, i.e. a larger device. An accurate calculation of synchrotron radiation is beyond the scope of this study. We have set $Z_{eff} = 1.5$ in the Bremsstrahlung

radiation calculation. The fusion power is calculated using rate coefficients from Ref. [34]. Furthermore have varied the edge temperature to maximize the fusion power produced by each equilibrium. Notice the reactor cases presented here do not directly contain the parameter τ_E/τ_p . Rather these cases assume that the pressure profile is limited to the marginal $pV^\gamma = \text{constant}$ profile which determines the energy confinement, that the tritium is removed sufficiently quickly that D-T fusion events only occur during the slowing down of the energetic tritons and that the deuterium fraction is consistent with $Z_{eff} = 1.5$.

The plasma parameters are shown in Table 2. We observe a peak local beta (ratio of plasma pressure to equilibrium magnetic field pressure) of $\beta_{max} \sim 3.1$ and the peak pressure $p(R_p)=5.4$ MPa. The β reduced magnetic field at the pressure peak is ~ 2.1 T which is relatively high due to the high aspect ratio of the floating coil (compare with the low aspect ratio D-T design discussed below). Since fusion power $\propto \beta^2 B^4$ the field is an important determinant of power production. Assuming that each triton is replaced by a ^3He the D-D and D- ^3He reactions (Eq. 1) would indicate 5.6% of the power is carried out by the 2.45 MeV neutrons. Assuming that the tritons cannot be removed before they slows down we add to the neutron power the 14.1 MeV D-T neutrons that are generated during the slowing down process. Table 2 indicated a neutron power is 34 MW at 2.45 MeV and 14 MW at 14.1 MeV which is equivalent to 7.9% of the total fusion power.

The total energy stored in the plasma $W_P \sim 2.9$ GJ so the effective energy confinement is $\tau_E^{global} = 3/2 \int (n_i T_i + n_e T_e) d^3r / (0.94 * P_{fus}) \sim 5.1$ s. We can formulate a local energy confinement time $\tau_E(\psi) = 3/2 p / (P_{fus} - P_{Brem})$ and compare it to a classical transport time, $\tau_{cl} = L^2 / \chi_{cl}$, with χ_{cl} the classical thermal diffusivity and L a characteristic temperature scale length given by $L = (d \ln T / dR)^{-1}$. The drive for the convective cells occurs in the region just beyond the pressure peak and in this region $\tau_{cl} / \tau_E|_{DD}(R \gtrsim R_p) \sim 20$ which indicates that additional energy transport must be present to balance

the local fusion heat deposition. This provides a measure of the energy transport associated with the convective flows. For $R \gtrsim R_p$ the additional energy transport mechanism is expected to derive from non-local transport driven by convective flows.

The pressure profile as a function of the midplane radius is shown in Fig. 3. The coil is located between $R=8.3$ m and 9.7 m. Figure 3 also shows the fusion power density and Bremsstrahlung radiation along the outer midplane. Notice that the energy transport provided by convective cells is necessary to transport power from the region of strong fusion power generation to the region of strong Bremsstrahlung radiation so as to maintain the critical gradient pressure profile (which has been clamped due to the stability requirements for MHD interchange modes).

3.1 Floating Coil Design

The floating coil consists of a winding pack surrounded by a cryostat that provides both thermal and neutron shielding. For steady state operation the floating coil must include an internal refrigerator in order to maintain the superconductor at a low temperature. For such a design it is critical to minimize the power deposited into the superconducting coil from volumetric neutron heating as it is inefficient to extract heat from the cold coil (~ 70 °K) and deposit it on the hot outer surface of the coil

The 3-D geometry of a floating toroidal coil is sufficiently complex that we have opted for utilizing a Monte-carlo code, MCNP4C [35] to estimate neutron power deposited into the superconductor and the shield. In this calculation the winding pack and cryostat/shield are approximated by a series of nested circular tori. For the calculation of neutronic properties we assume that the coil contains BSCCO high T_C superconductor and it is located within a simple segmented cryostat/shield. We have divided the shield into two annular toroidal sections: an outer region of tungsten-boride and an inner region of boron carbide. The plasma flux surfaces are approximated by

Bounding Toroid	D-D reactor (A & B)		D-T Ignition	
	R_{major} (m)	R_{minor} (m)	R_{major} (m)	R_{minor} (m)
BSCCO Coil	9	0.186	1.5	0.113
B_4C shield, Inner surface	9.15	0.206	1.5	0.13
B_4C shield, Outer surface	9.15	0.406	1.65	0.38
WC shield, Inner surface	9.15	0.406	1.5	0.13
WC shield, Outer surface	9.15	0.701	1.65	0.38
Plasma, Inner Boundary	9.19	0.78, 0.77†	1.70	0.47, 0.44 †
Plasma, Outer Boundary	9.50	1.28, 1.08†	1.92	0.76, 0.59 †

Table 3: Coil and Plasma geometry.

† Horizontal and vertical radii for elliptic cross section tori.

	D-D Reactor	D-T Ignition
Fraction neutron power deposited in coil	5.4×10^{-5} #	0.0045, 0.0039†
Fraction neutron power deposited in shield	0.21 #	0.102, 0.125 †
Fraction Bremsstrahlung to coil surface	0.237	0.43
$P_{brem}(out)/P_{brem}(in)$	2.57	2.47
Neutron power to Shield (MW) **	14.1	
Bremsstrahlung to Coil Surface (MW) **	110	
Plasma power to Coil Surface (MW) **	27	

Table 4: Monte-carlo results

Combination B_4C /WB shield (Table 3).

† Respective B_4C and WB shields.

** High power option (A)

nested elliptic cross section tori and the neutrons are assumed to be emitted by plasma that is contained between two flux surfaces that are chosen so as to contain 80% of the generated fusion power. The neutron and Bremsstrahlung photon sources are approximated as being uniformly distributed within the fusing plasma. Table 3 indicates the chosen geometry of the plasma and the coil. The Monte-carlo calculations follow 2×10^5 to 8×10^5 particles and use the splitting technique to improve statistical accuracy.

The calculation of a conceptual reactor summarized in Table 3 indicates that $\sim 24\%$ of neutrons and photons will impinge directly on the coil. Since most of the plasma volume is located near the outer mid-plane the coil will be unevenly irradiated by the neutrons and photons which results in a higher power flux to the outer facing surface of the coil as compared with the inner facing surface. The power flux distribution is shown in Fig 5. Notice that the outer heat flux is 2.57 times the inner flux and approximately 65% of the power flux impinges on the outward facing surface of the torus (defined by $|\theta| < \pi/2$ with θ the poloidal angle the coil surface makes with the outer mid-plane). Approximating the first wall of the reactor by a right circular cylindrical vacuum chamber with 30 m radius and 20 m height yields the result that 25.9% of the radiated power will impinge directly on the outer radial surface and 25.2% on each of the top and bottom planes.

The mid-plane magnetic field of a floating coil is always much higher on the inside as compared with the outside of the coil. The surface of the cryostat follows a magnetic field flux surface and, as a result, there is less room for neutron and thermal shielding on the inner region of the cryostat compared to the outer. Thus, although the neutron flux per surface area impinging on the coil surface from the outside is higher than from the inside, the heat entering the cold winding pack is dominated by the flux generated in the inside which can penetrate the thinner shield.

The temperature of the outer surface of the coil is determined by the requirement that the heat deposited on the coil surface or within the coil

volume be radiated via black body radiation from the surface of the coil:

$$A_T \sigma T_{surf}^4 = \alpha_1 P_{rad} + \alpha_2 P_{neut} + \alpha_3 P_{conv} \quad (11)$$

with P_{rad} , P_{neut} , P_{conv} respectively the total radiated power, neutron power and convected power leaving the plasma and $A_T = 253 \text{ m}^2$ is the surface area of the floating coil. The α_i coefficients represent the fraction of this power deposited on/into the floating coil. From the Monte-carlo calculations we find $\alpha_1 = 0.237$ and $\alpha_2 = 0.207$. Assuming that half of the power leaving the plasma as conducted and convected particle energy (i.e. the non-radiated power) goes inwards toward the floating coil and that a recycling gas blanket forms at the coil surface which radiates half of the power flowing toward the coil we estimate that $\alpha_3 \approx 1/4$. Equation (11) indicates that the outer surface of the coil will rise to an average temperature, $T_{surf} \approx 1,800 \text{ }^\circ\text{K}$.

The low thermal efficiency associated with maintaining the superconductor at a low temperature will require that a great deal of attention be focused on the design of the floating coil shield. The shield must protect the coil from both low (2.45 MeV) and high (14.1 MeV) energy neutrons. To get a rough estimate of the difficulty of this problem we have considered several simple shield designs including shields made up of WC , B_4C , or the segmented combination shown in Table 3. The best results (least direct heating of superconductor) were found for the latter segmented shield which indicates a direct deposition into the coil of 1.4 KW from high energy and 2.2 KW from low energy neutrons. The low level of heating from the 14 MeV neutrons requires the removal of thermal tritium as we have assumed.

In total we find that there is 137 MW of power deposited into the surface of the coil (DD study in Table 4). If we thermally isolate the outer and inner shells we can use the temperature difference to drive a refrigerator. Assume the inner, cooler half of the torus is at a temperature T_c and the outer, hotter half at T_h . The refrigerator efficiency is $\eta_r = (1/\epsilon)(T_c - T_{sc})/T_{sc} \approx T_c/\epsilon T_{sc}$ with T_{sc} the temperature of the superconductor and $\epsilon \sim 0.5$ will be assumed to be the reduction of the efficiency below Carnot. Assuming that we can use

the temperature difference to generate electric power to run the refrigerator, the efficiency of this process is $\eta = \epsilon(T_h - T_c)/T_h$. The radiation balance from the two surfaces determines the relative temperatures as follows:

$$\begin{aligned} A_h \sigma T_h^4 &= P_h + P_{shield} - \frac{\eta_r(T_c)}{\eta(T_c, T_h)} P_{sc} \\ A_c \sigma T_c^4 &= P_c + \frac{\eta_r(T_c)}{\eta(T_c, T_h)} P_{sc}. \end{aligned} \quad (12)$$

For $P_h=85$ MW of power to outer side of the coil, $P_c=52$ MW to the inner side, $P_{shield}=14$ MW neutron heating of the shield, $P_{sc}=3.65$ KW of direct neutron heating to the superconductor and we find $T_h = 1925$ $^{\circ}K$ and $T_c = 1641$ $^{\circ}K$.

4 D-T Ignition Experiment

The D-T fusion reaction produces 80% of the fusion power output in energetic (14.1 MeV) neutrons and it is difficult to adequately shield the superconductor within the floating coil. However since the D-T fusion reaction rate coefficient [34] is much larger than the D-D coefficient, a small experiment testing ignition in a dipole configuration is worth considering as a first step toward a dipole based D-D power source. In this application the floating ring would be minimally shielded and once ignition occurs the ring would be permitted to warm up to a level at which the coil will quench. We have found that that a pulsed ignition experiment could permit greater than 5 minutes of float time for the coil.

D-T ignition can be achieved in a relatively small dipole experiment. One such conceptual design is indicated in Table 1 and the plasma parameters, consistent with the high- β equilibrium are listed in Table 2. We find that in this relatively small device D-T fusion will generate 15.4 MW of total power or 12.3 MW of neutron power. This power level is small compared to proposed tokamak-based ignition experiments and indicates that ignition

Shield Material	Fraction to SC	Fraction to Shield	Float time (m)
WC	0.0031	0.127	8.6
B_4C	.00045	0.102	7.1
LiH	0.0054	0.178	6.4

Table 5: D-T Study for coil with WC, B_4C and LiH shields: fraction of neutron power to superconductor, fraction neutron power to shield, float time.

in a dipole would require a relatively small facility. As in the D-D case discussed above classical confinement exceeds the implied energy confinement time ($\tau_{cl}/\tau_E|_{DT}(R \gtrsim R_p) \sim 3$) in the absence of convective cells.

Monte-carlo calculations have been performed for the the coil and shield geometry listed in Table 3. The shielding of energetic 14.1 MeV neutrons is difficult and a study was performed to compare several different shield materials. Results of the study are shown in Table 5 for three shields, WC, B_4C and LiH respectively. With a B_4C shield there will be 55.5 KW of direct neutron heating to the superconducting coil and 1.57 MW to the shield. With a WC shield direct neutron heating of the conductor is reduced to 47.5 KW with 1.26 MW to the shield.

Considering D-T fusions we find that 43% of neutrons and photons impinge on the $24.7 m^2$ surface of the floating coil. This leads to 204 KW of Bremsstrahlung surface heating in addition to 604 KW of convective power that flows onto the coil surface. With a B_4C (WC) shield 10.2% (12.5%) of the neutron power is deposited into the shield and 0.45% (0.39%) is deposited into the coil.

The BSSCO superconductor has a specific heat of $\sim 0.26 J/(g-^0K)$. Taking account of the direct neutron heating of the superconductor we can estimate the float time of the coil assuming that the temperature of the coil can rise from 20 to 45 0K . The results of this calculation, shown in Table 5, indicate a float time of 6 to 9 minutes. Thus we can estimate that once ig-

nited a dipole experiment can have a burn time of greater than 6 min, a time interval which greatly exceeds any of the characteristic plasma times, i.e. the slowing down time, the energy confinement time or the particle confinement time.

5 Discussion

We have provided a conceptual design based on accurate equilibria and neutron and photon calculations. However, since a dipole is a radically different fusion confinement concept than those systems that gain stability due to rotational transform, (i.e. a tokamak, stellarator, etc.) there remains many interesting questions relating to both physics and technology that must be answered. While there is a history of research in supported dipole confined laboratory plasmas [36, 38], the first levitated dipole experiment is now being built [4].

We have assumed that the levitated dipole device provides a sufficient energy confinement for ignition. The ability to ignite the device without violating the critical pressure gradient (set by MHD interchange modes) determines the size of the device. In the self-sustained, ignited plasma, convective cells are assumed to be present which give rise to a rapid particle circulation and to a sufficient energy transport to maintain the pressure gradient at close to its critical value. The assumption that turbulent transport does not substantially degrade confinement is based on theoretical studies [30, 31]. The experimental verification of turbulence free plasma operation in the presence of convective flows that do not transport significant energy remains to be examined experimentally. In planetary magnetospheres as well as in supported dipole experiments the primary loss mechanism for bulk plasma is flow along field lines into the planetary poles or coil supports and cross-field transport is difficult to observe.

We have assumed that the plasma is heated up to ignition by traditional

methods, i.e. neutral beams and RF. If it is important to utilize a particular heating profile in order to avoid instability before ignition is achieved the heating system may require a combination of heating methods.

When the outer flux tube is determined by an magnetic seperatrix containing a field null the stability criterion given by Eq. (6) no longer limits the edge pressure gradient ($\nabla p \rightarrow \infty$ as $U \rightarrow \infty$ [37]). This suggests the possible formation of an edge pressure pedestal which could reduce the size of the proposed device.

In the inner plasma which is embedded in a magnetic field exhibiting “good curvature” (between the pressure peak and the floating coil), η ($= d \ln T / d \ln n$) can be negative and theory indicates the possibility of low frequency instability [30, 31, 32]. The level of transport for such modes depends on the non-linear saturation mechanism. Transport of energy towards the ring is important for determining the heating of the internal ring. The relative transport of plasma energy inwards toward the ring and outwards towards the vacuum chamber wall will determine the location of the pressure peak which in turn determines the energy production of a reactor.

We have proposed to pump the tritium as it convects from the core out to the plasma edge (otherwise it would circulate back into the core). As the field at the plasma edge is low ($B_{edge} < 0.1$ T) we might use cyclotron heating to eject tritons with large gyro-radii. If we heat at the cyclotron frequency of tritium and the cyclotron layer occurs close to an edge limiter the fundamental frequency layer for deuterium and alpha particles may be arranged to occur beyond the confinement zone since deuterium and alphas would be resonant at 2/3 of the field of the tritium cyclotron resonance. Similarly the fundamental cyclotron frequency layer for ^3He occurs at 1/2 of the tritium resonance field and for protons it occurs at 1/3 the field. Higher harmonic resonances do occur deeper into the confined plasma but cyclotron heating of higher harmonics is weak for the low edge temperatures envisioned. The antenna heating/pumping arrangement could utilize near-field heating

to limit field penetration. The efficiency of this or other possible pumping techniques will be explored in future publications.

The design of the floating coil presents a substantial challenge. Advances in high temperature superconductors may ease some of the constraints. The coil requires a refrigerator that can eject heat at above 1600 $^{\circ}\text{K}$ and Furthermore the refrigerator must be powered by a generator that operates between the high temperatures of the outer shell of the floating coil, i.e. between 1500-1600 $^{\circ}\text{K}$ and 1800-1900 $^{\circ}\text{K}$. In this regard we have presented estimates based on a Carnot cycle but the efficiency can be improved through the use of thermoelectric generators.

We have assumed that the synchrotron radiation is reflected at the vacuum chamber wall and reabsorbed in the plasma. Alternatively it can be guided beyond the first wall and converted directly into electric power by rectennas.

The first wall of the surrounding vacuum chamber will absorb the fusion power that flows onto it as surface heating. The surface area of the vacuum chamber wall is $> 5000 \text{ m}^2$ and the power loading is $< 0.1 \text{ MW}/\text{m}^2$. The cooling of the large plasma facing surface can be challenging. Systems can be devised to increase the wall loading. For example we can permit a part of the wall to run at a hot ($\sim 1000 \text{ }^{\circ}\text{K}$) temperature so that it will re radiate the surface heat. The heat may then be collected in a smaller region (at 500 – 600 $^{\circ}\text{K}$) and at a higher power density. The large vacuum chamber can be built under ground with the walls anchored into the surrounding medium so as to support the vacuum stresses.

The storage of the of the tritium that is removed from the discharge during its 12.3 year half life will require the safe storage of 100 to 200 Kg of tritium. Most tritium storage systems (i.e. for DT fusion applications) require the ability to recover the tritium quickly when it is needed and a favored storage medium for tritium is a uranium bed. For the dipole reactor the requirement is somewhat different as we want to bind the tritium in a

stable system and only extract the ^3He decay product. One suggestion is to use titanium for tritium storage [39]. Indications are that such systems can get a T/Ti ratio of 2/1 and that storage of quantities like 100-200 Kg does not appear to be unreasonable. Of course strategies need to be worked out for ^3He fueling during the first decade of operation.

6 Conclusions

We have proposed a novel approach for a fusion power source, based on an alternative fuel cycle which we call “He catalyzed D-D”. Due to the possibility of high beta and high energy confinement with low particle confinement we find that a levitated dipole is ideally suited as a D-D based power source. A levitated dipole device would be intrinsically steady state and extract power as surface heating, permitting a thin walled vacuum vessel and eliminating the need for a massive neutron shield. The magnetic field would be produced by a coil that is internal to the plasma and the plasma pressure falls off as the magnetic field falls off leading to a good utilization of the field. Therefore although the vacuum chamber envisioned is relatively large this does not lead to an unreasonably large magnetic field energy. Compared with a tokamak, there are no interlocking coils. The device has only one difficult coil and coil replacement would be relatively straight forward.

From Tables 1 and 3 we observe that the ratio of plasma stored energy to magnet energy is $R_W = 0.096$ whereas for an advanced tokamak reactor it is several times smaller: for the ARIES AT [40] advanced tokamak conceptual reactor study $W_B = 45$ GJ, $W_P = 0.75$ GJ and therefore $R_W = 0.017$. The ratio ($R_W^{dipole} / R_W^{aries} \sim 5.7$) indicates a substantially better utilization of magnetic field energy in a dipole which results from the high average beta that a dipole can support. Although the Aries AT wall loading (3.3 MW/m² from neutrons) exceeds the dipole reactor wall loading (photons and particles) by a factor of 40, the mass power density [41], i.e. the power per unit volume

of structure (first wall + coil) which we estimate to be 1.7 MW/m^3 for the dipole is comparable to the mass power density of Aries, estimated to be 1.5 MW/m^3 (thermal power= 2 GW , system volume= 1300 m^3). The low surface heat flux leads one to expect that the first wall will not suffer damage from either neutron or surface heat flux and that the divertor heat flux will not pose a problem.

The D-T study presented here indicates that an important ignition test experiment could be performed in a relatively small facility. Additionally tritium may be used to ignite the burn in a D-D reactor. The comparison of the small D-T ignition test and the large D-D power source is illustrative of the scaling of a dipole configuration. For the power source, we have chosen a large aspect ratio coil so as to raise the outboard field and to permit more space for the shielding of the inner region of the shield.

The LDX experiment, presently under construction [4] will focus on many of the questions that have been raised.

Acknowledgements

The authors would like to thank Dr. W. Nevins (LLNL) for supplying the fusion cross-section code. We would like to thank Dan Berkley (Bates College) for valuable assistance in running the MCNP code. This work was supported by the US DoE.

Figure Captions

1. Lawson criteria for various fusion reactions. The solid red line is for D-T, the blue line is D- ^3He , the dashed line shows catalyzed D-D, and the black line is He catalyzed D-D.
2. Beam-plasma fusion probability for a 1 MeV triton slowing down in a warm deuterium plasma.

3. Pressure, fusion power density and Bremsstrahlung profiles on the dipole midplane.
4. Plasma equilibrium for $R_c=9.7$ m, $R_p=10.15$ m, $R_w=30$ m and the edge plasma pressure $p(R_w)=400$ Pa which yields a peak β value of $\beta(R_p)=3.1$.
5. Surface heat flux as a function of poloidal angle of the the coil.

References

- [1] W.M. Nevins, *Journal of Fusion Energy* **17**, (1998) 25.
- [2] A. Hasegawa, *Comments Plasma Phys. Controlled Fusion*, **1**, (1987) 147.
- [3] Hasegawa, A., Chen, L., Mauel, M., *Nucl. Fusion* **30**, (1990) 2405.
- [4] J. Kesner, L. Bromberg, D.T. Garnier, M.E. Mauel, "Plasma Confinement in a Magnetic Dipole", 17th IAEA Fusion Energy Conf, Paper IAEA-F1-CN-69-ICP/09 Yokohama, Japan (1998), *Fusion Energy 1998*. (Proc. 17th Int. Conf. Yokohama, 1998) (Vienna: IAEA) CD-ROM file IAEA-CSP-1/C and <http://www.iaea.org/programmes/ripc/physics/start.htm>.
- [5] M.N. Rosenbluth and C.L. Longmire, *Ann. Phys.* **1**, (1957) 120.
- [6] I.B. Bernstein, E. Frieman, M. Kruskal, R. Kulsrud, *Proc. R. Soc. Lond. A* **244** (1958) 17.
- [7] V.P. Pastukhov, *Plasma Physics Reports* **26**, (2000) 529.
- [8] V.P. Pastukhov and N.V. Chudin, *Plasma Physics Reports* **27**, (2001) 907.
- [9] J. Tonge, J.N. Leboeuf, C. Huang, J.M. Dawson, *Phys. Plasmas* **10**, (2003) 3475.
- [10] W. Kuan, M.A. Abdou and R.S. Williams, *Fusion Technology* **28**, (1995) 664.
- [11] V.I. Khvesyuk and A.Yu Chirkov, *Plasma Phys. Control Fusion* **44**, (2002) 253.
- [12] E. Teller, A. Glass, T.K. Fowler, J. Santarius, *Fusion Technology* **22**, (1992) 82.
- [13] L. Wittenberg, J.F. Santarius and G.L. Kulcinski, *Fusion Technology* **10**, (1986)167.
- [14] J.S. Lewis *Space Power*, **10** (1991) 363.
- [15] M.E. Sawan, S.J. Zinkle, J. Sheffield, "Impact of Tritium Removal and He-3 Recycling on Structure Damage Parameters in a D-D Fusion System," UWFDM-1176 (April 2002) [presented at the 6th International Symposium on Fusion Nuclear Technology, 7-12 April 2002, San Diego CA; published in *Fusion Engineering and Design*, vol. 61-62, pp. 561-567 (2002)].
- [16] B.A. Trubnikov, *Particle Interactions in a Fully Ionized Plasma*. Reviews of Modern Physics, Vol. 1 (Consultants Bureau, New York, 1965), p 105.
- [17] G.H. Miley, H. Towner and N. Ivich, *Fusion Cross-section and Reactivities*, Rept. C00-2218-17 (Univ of Illinois, Urbana, Ill, 1974).
- [18] B. Lehnert, *Plasma Physics* **10** (1968) 263.
- [19] D.T. Garnier, J. Kesner, M.E. Mauel, *Phys. Plasmas* **6**, (1999) 3431.
- [20] A.N. Simakov, P.J. Catto, S.I. Krasheninnikov, J.J. Ramos, *Phys. Plasmas* **7**, (2000) 2526.

- [21] A. Simakov, P. Catto, R.J. Hastie, J.J. Ramos, *Phys Plasmas* **9**, (2002) 4985.
- [22] J. M. Dawson, H. Okuda and R. Carlile, *Phys. Rev. Lett.* **27**, (1971) 491.
- [23] H. Goede, D. Humanic, J. Dawson, *Phys Fluids* **26**, (1983) 1812.
- [24] A. Hassam, R. Kulsrud, *Phys Fluids* **22**, (1979) 2097 .
- [25] J. Kesner, D.T. Garnier, *Phys. Plasmas* **7**, (2000) 2733.
- [26] A.M. Rey and A.B. Hassam, *Phys. Plasmas* **8**, (2001) 5151.
- [27] J. Kesner, *Phys. Plasmas* **10**, (2003) 908.
- [28] V.P. Pastukhov and N.V. Chudin, “Non-Linear 2D Convection and enhanced Cross-Field Transport Near the MHD Instability Threshold” 19th IAEA Fusion Energy Conf, Paper IAEA-TH/2-5, Lyon, France, (2002), *Fusion Energy 2002* (Proc. 19th Int. Conf. Lyon, 2002) (Vienna: IAEA) CD-ROM file IAEA-CSP-19/CD and <http://www.iaea.org/programmes/ripc/physics/fec2002/html/fec2002.htm>.
- [29] J. Kesner, *Phys. Plasmas* **7**, (2000) 3837 .
- [30] J. Kesner, R.J. Hastie, *Phys. Plasmas* **9**, (2002) 395.
- [31] A. Simakov, P. Catto, R.J. Hastie, *Phys. Plasmas* **8**, (2001) 4414.
- [32] A. Simakov, R.J. Hastie, P. Catto, *Phys. Plasmas* **9**, (2002) 201.
- [33] T.P. Sheahen, *Intro to High Temperature Superconductivity* (Plenum Press, New York (1994)).
- [34] H.S. Bosch and G.M. Hale, *Nuclear Fusion* **32**, (1992) 611.
- [35] J.F. Briesmeister, Ed., *MCNP4C: Monte Carlo N-Particle Transport Code System*, Oak Ridge National laboratory Report CCC-700 (2000).
- [36] B. Lehnert, *Plasma Physics and Controlled Nuc Fus Res, 1971*, (International Atomic Energy Agency, Vienna 1971) p59.
- [37] T. Hellsten, *Physica Scripta* **13** (1976) 313.
- [38] H. P. Warren and M. E. Mauel, *Phys. Rev. Lett.* **74** (1995) 1351.
- [39] D.K. Sze, UCSD, private communication, 8/2003.
- [40] F. Najmabadi, S.C. Jardin, M. Tillack , L.M. Waganer and the AIRIES Team, “ARIES-AT: An Advanced Tokamak, Advanced Technology Fusion Power Plant”, 19th IAEA Fusion Energy Conf, Paper IAEA-CN-77-FTP2/15, Lyon, France, (2002), *Fusion Energy 2002* (Proc. 19th Int. Conf. Lyon, 2002) (Vienna: IAEA) CD-ROM file IAEA-CSP-19/CD and <http://www.iaea.org/programmes/ripc/physics/fec2002/html/fec2002.htm>. To be published in *Fusion Eng. and Design* (2003) .

- [41] R.A. Krakowski, R.L. Miller, J.G. Delene, “Directions for improved fusion reactors”, Fusion Reactor Design and Technology 1986, Proceedings of the Fourth Technical Committee Meeting and Workshop, STI-PUB-754. (1987) vol.1, p 265-83. Detailed parameters from <http://aries.ucsd.edu/miller/AT31002/output.html>.

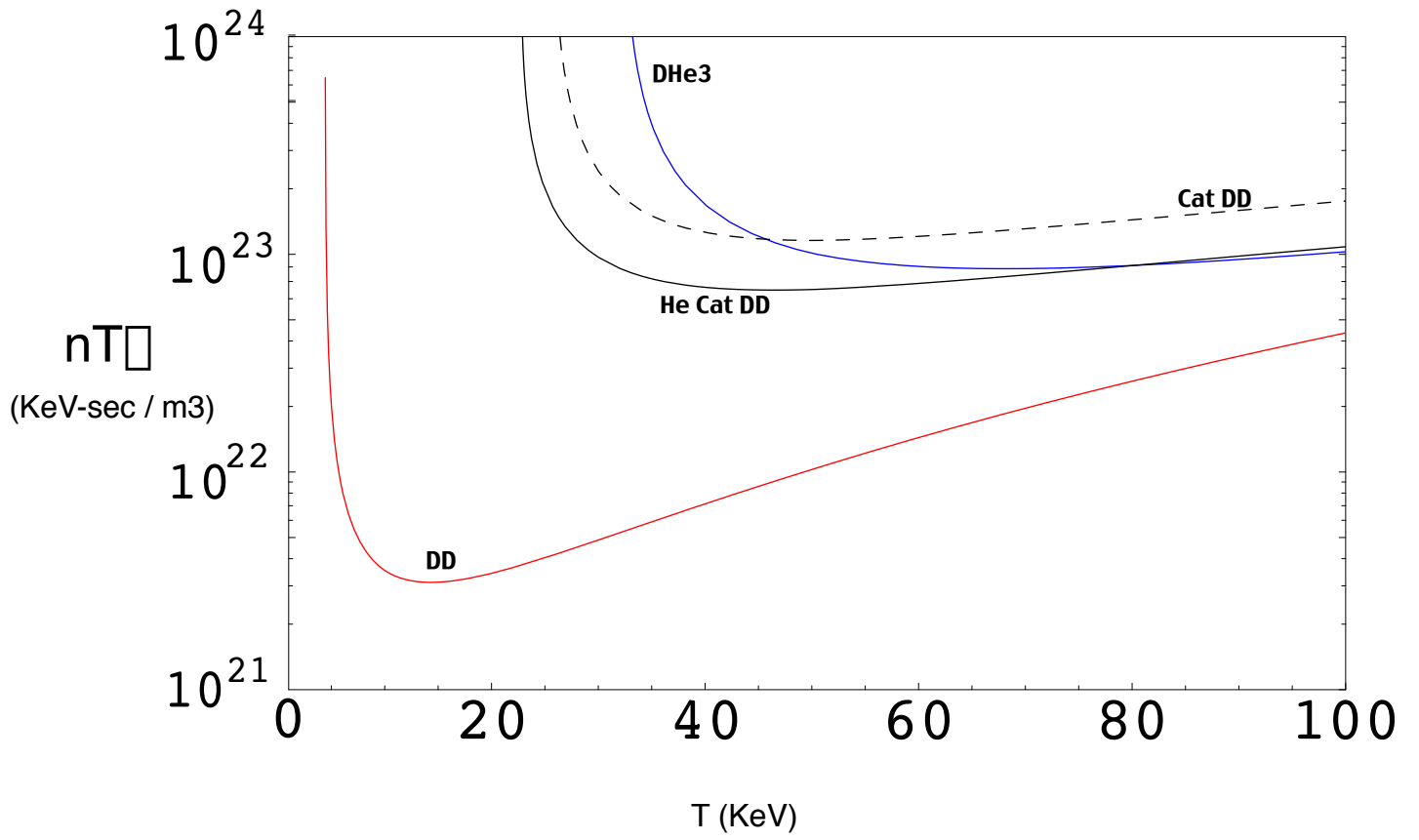
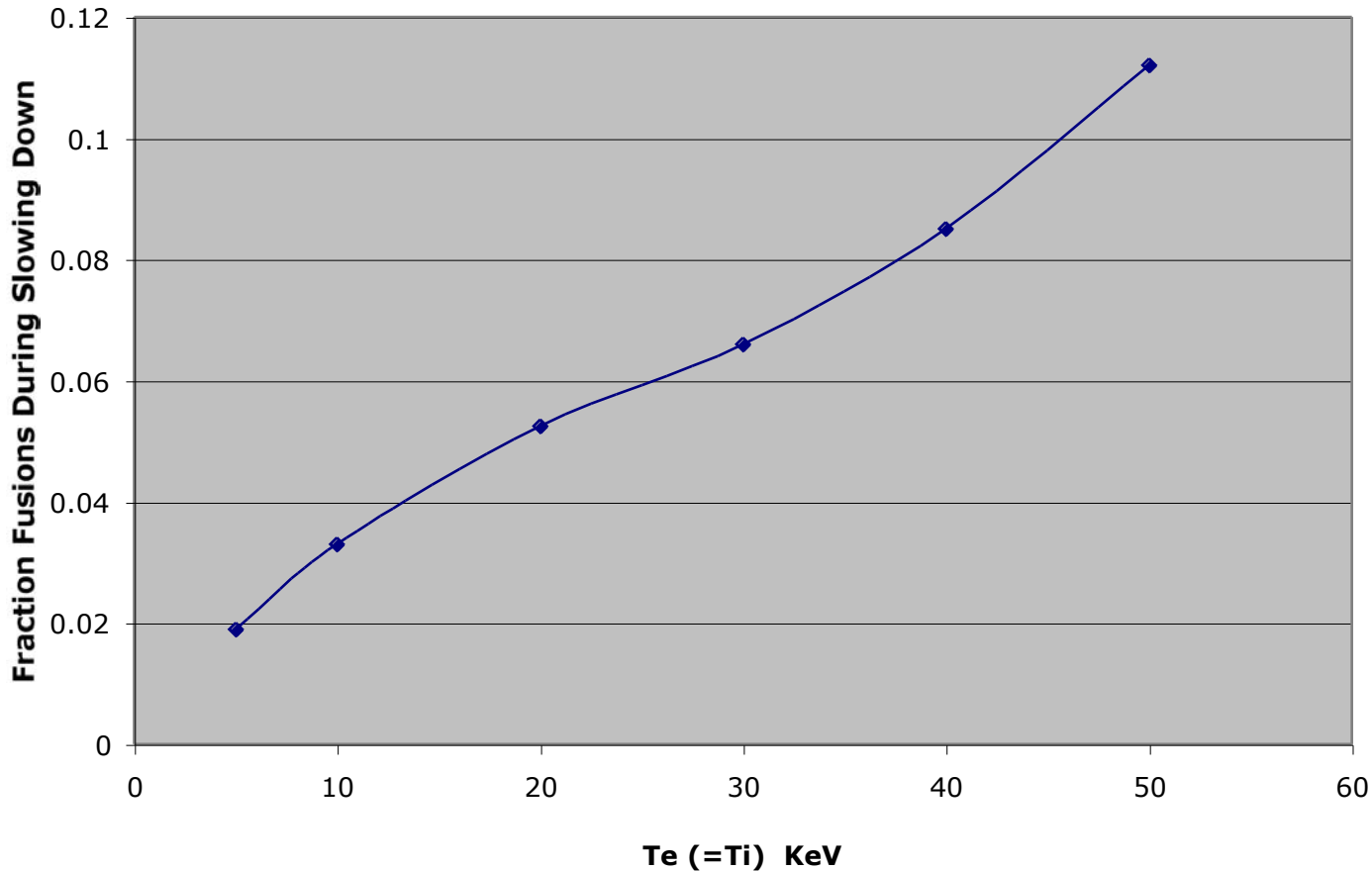
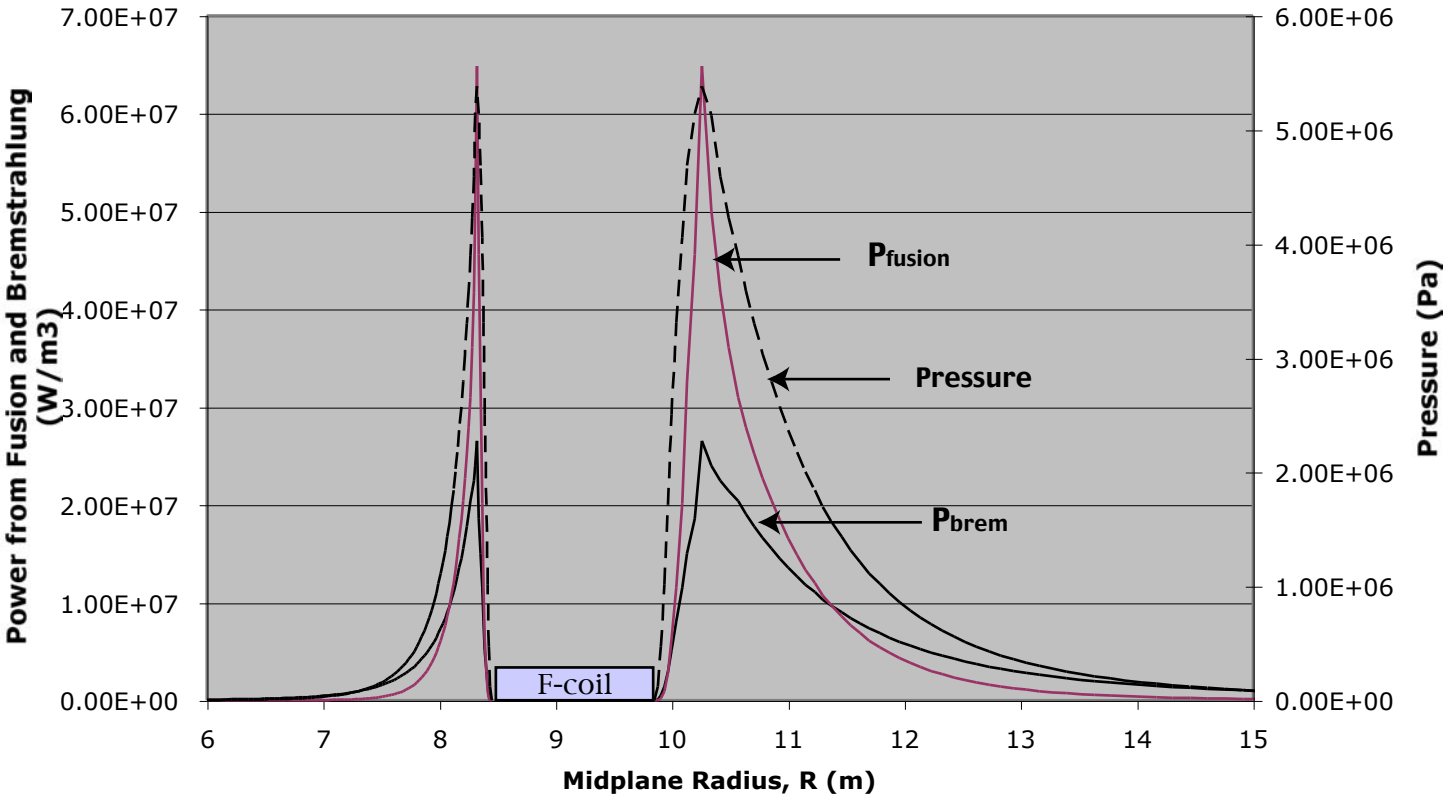


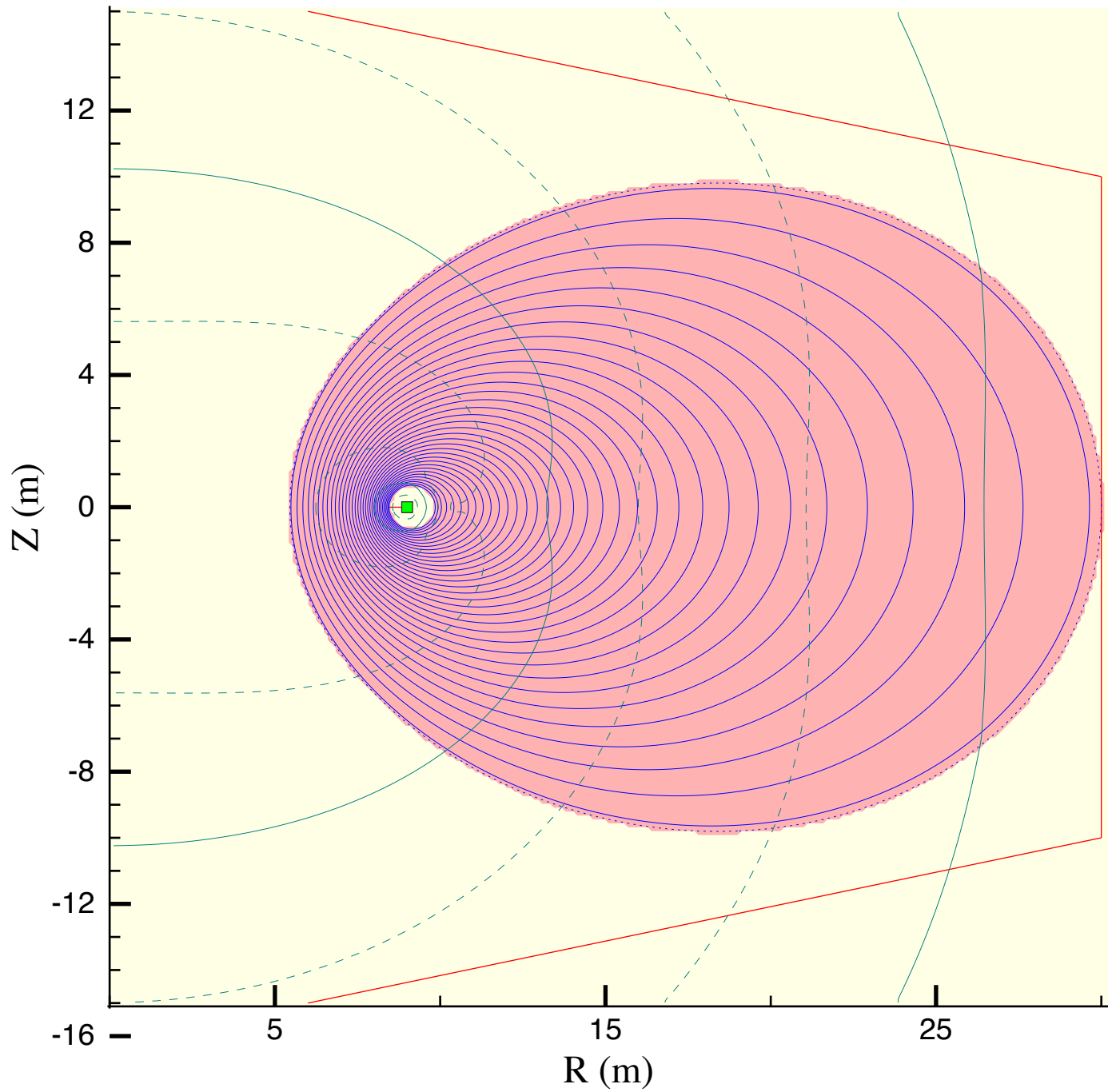
Fig. 1

Fusion Probability; 1.01 MeV triton in Deuterium Plasma



Midplane Profiles





Angular Bremsstrahlung Heating of Coil ($\theta = 0$ on outer midplane of coil)

